Magnetic and Transport Properties of Ferromagnet $NdCrSb_3$

Laura Deakin, Michael J. Ferguson,† and Arthur Mar*

Department of Chemistry, University of Alberta, Edmonton, Alberta, Canada T6G 2G2

John E. Greedan* and Andrew S. Wills

Brockhouse Institute for Materials Research, McMaster University, Hamilton, Ontario, Canada L8S 4M1

Received December 18, 2000. Revised Manuscript Received January 29, 2001

$NdCrSb_3$, a compound containing alternating layers of Nd and Cr atoms in its structure, undergoes two ferromagnetic ordering transitions. At 107.8 K, ferromagnetic ordering of the Cr moments occurs; at 12.7 K, ferromagnetic ordering of the Nd and Cr moments occurs. Neutron diffraction studies place the magnetization axis for the ordered Cr moments along [010], and for the coupled Nd and Cr moments along [100]. These transitions are also observed in the temperature dependence of the dc magnetization, and as maxima in the χ'_{ac} and χ''_{ac} magnetic susceptibilities. Hysteresis loops at 2 and 40 K revealed saturation magnetization values of 3.70 and 2.37 μ_B/f.u. and coercive fields of 2100 and 400 Oe, respectively. The saturation magnetization of 3.7 μ_B at 2 K is the same as that determined from neutron diffraction studies. Both ferromagnetic ordering transitions are manifested as kinks in the temperature dependence of the electrical resistivity. Field-dependent resistivity measurements made between 2 and 130 K indicate negative magnetoresistance behavior with values up to −13%.

Introduction

While current interest on ternary rare-earth transition-metal antimonides is concentrated (perhaps excessively) on the filled skutterudite variants REM_4Sb_{12} because of their potential as improved thermoelectric materials,[1] emerging results suggest that other members also exhibit interesting magnetic and electrical behavior. Measurements on even the simple binary rare-earth diantimonides $RESb_2$ have only recently been carried out and point to a wide range of physical properties, such as high magnetoresistance, possessed by these quasi-two-dimensional compounds.[2] These results provide incentive for studying the effect of including a transition metal on such properties in ternary antimonides that retain an essentially two-dimensional electronic structure.

In the series of ternary rare-earth antimonides $RECrSb_3$ (RE = La−Nd, Sm, Gd−Dy), single-crystal structures have been determined for two members, $LaCrSb_3$ and $CeCrSb_3$.[3,4] The structure of $RECrSb_3$ (Figure 1) can be regarded as being built up by the insertion of a "CrSb" layer into the structure of $RESb_2$ (RE = La−Nd, Sm),[5] which in turn is composed of square sheets of Sb atoms and layers of Sb_2 pairs separated by the RE ions: $^2_\infty[RESb_2] + {}^2_\infty[CrSb] = {}^3_\infty[RECrSb_3]$. The layers are stacked along the [100] direction. Previously, neutron diffraction studies revealed that $LaCrSb_3$ displays itinerant electron ferromagnetism, with a T_C of 125 K arising from ordering of the Cr moments.[6] We have now investigated the electronic properties of another member, $NdCrSb_3$, containing a magnetic rare-earth component, to examine the effect of interactions between the rare-earth and transition-metal moments. Other studies have suggested the presence of either an antiferromagnetic[7,8] or canted antiferromagnetic[9] spin structure of the RE and Cr moments in $RECrSb_3$ for RE = Ce, Pr, Nd. Neutron diffraction methods are the most appropriate for determining the detailed magnetic structure, which is reported here for $NdCrSb_3$. The electrical resistivity and magnetoresistance behavior of $NdCrSb_3$ are also described.

Experimental Section

Synthesis. Samples of $NdCrSb_3$ for neutron diffraction and magnetic susceptibility measurements were prepared from reaction of powders of the elements (Nd, 99.9%, Cerac; Cr,

* To whom correspondence should be addressed.
† Current address: Steacie Institute for Molecular Sciences, National Research Council of Canada, Ottawa, ON, Canada K1A 0R6.

(1) Sales, B. C.; Mandrus, D.; Williams, R. K. *Science* **1996**, *272*, 1325.
(2) Bud'ko, S. L.; Canfield, P. C.; Mielke, C. H.; Lacerda, A. H. *Phys. Rev. B* **1998**, *57*, 13624.
(3) Ferguson, M. J.; Hushagen, R. W.; Mar, A. *J. Alloys Compd.* **1997**, *249*, 191.
(4) Brylak, M.; Jeitschko, W. *Z. Naturforsch. B* **1995**, *50*, 899.
(5) Wang, R.; Steinfink, H. *Inorg. Chem.* **1967**, *6*, 1685.
(6) Raju, N. P.; Greedan, J. E.; Ferguson, M. J.; Mar, A. *Chem. Mater.* **1998**, *10*, 3630.
(7) Leonard, M.; Saha, S.; Ali, N. *J. Appl. Phys.* **1999**, *85*, 4759.
(8) Hartjes, K.; Jeitschko, W.; Brylak, M. *J. Magn. Magn. Mater.* **1997**, *173*, 109.
(9) Leonard, M. L.; Dubenko, I. S.; Ali, N. *J. Alloys Compd.* **2000**, *303−304*, 265.

10.1021/cm001405l CCC: $20.00
Published on Web 03/09/2001

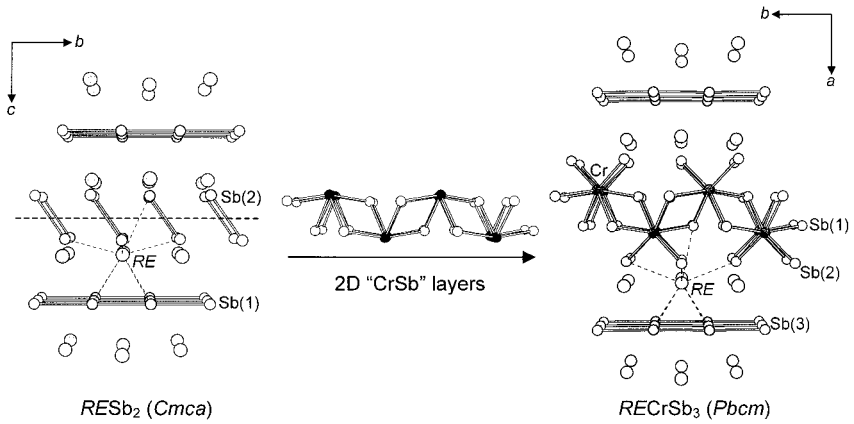

Figure 1. Structure of $RECrSb_3$ as a composite of $RESb_2$ (RE = La−Nd, Sm) and "CrSb".

99.95%, Cerac; Sb, 99.995%, Aldrich). The elements were loaded into fused-silica tubes (5-cm length, 10-mm i.d.) in a 1:1:3 ratio, which were then evacuated, sealed, and heated in a furnace at 630 °C for 1 day and 1000 °C for 4 days, and then cooled to 20 °C over 1 day. The products were analyzed by powder X-ray diffraction with the use of an Enraf-Nonius FR552 Guinier camera (Cu $K\alpha_1$ radiation, Si standard). The diffraction pattern revealed that the ternary compound $NdCrSb_3$, isostructural to $LaCrSb_3$, is the major phase present (>90%), with only weak reflections arising from a $NdSb_2$ impurity phase. Single crystals of $NdCrSb_3$ used for resistivity measurements were obtained from direct reaction of elements as above but involving a slow cooling from 1000 to 20 °C over 8 days. Elemental composition of selected crystals was confirmed by EDX (energy-dispersive X-ray) analysis on a Hitachi S2700 scanning electron microscope.

Magnetic Susceptibility. Magnetic data were measured on powders placed in a gel-cap sample holder with a Quantum Design PPMS 9T magnetometer/susceptometer between 2 and 300 K and in applied fields up to 9 T. ac magnetic susceptibility measurements were made with a driving amplitude of 1 Oe and frequencies between 10 and 1000 Hz. The magnetic susceptibility was corrected for the holder and the sample diamagnetism (Nd: -20×10^{-6}; Cr: -11×10^{-6}; Sb: -15×10^{-6} emu/mol).

Neutron Diffraction. Neutron diffraction data were collected on the C2 instrument of the DUALSPEC installation at the Chalk River Nuclear Laboratories and the Neutron Program for Materials of the National Research Council of Canada. The neutron wavelength was 2.3735 Å. The sample was sealed under helium in a vanadium can with an indium gasket and attached to the cold stage of a liquid helium cryostat. The temperature was controlled to within ±0.1 K. Rietveld analysis was performed using FULLPROF Version 3.5.[10]

Electrical Resistivity. The electrical resistivity of single crystals (typically $\approx 1.0 \times 0.1 \times 0.1$ mm^3) was measured by standard four-probe ac methods with a Quantum Design PPMS ac-transport controller (model 7100) between 2 and 300 K. A current of 0.1 mA and a frequency of 16 Hz were used. The resistivity was measured parallel to the needle axis (corresponding to the crystallographic *c* axis) of the crystals, which were mounted perpendicular to the applied field. After the crystals were cooled in zero field, the resistivity was measured under various applied fields upon warming.

Results and Discussion

Magnetic Structure. The magnetic susceptibility of $NdCrSb_3$, measured under zero-field-cooled (ZFC) and field-cooled (FC; 2 T cooling field) conditions as a function of temperature, is shown in Figure 2. The divergence between these curves below 120 K suggests ferromagnetic ordering of the Cr moments, at a temperature similar to that observed (125 K) in $LaCrSb_3$, where this magnetic structure has been established.[6] The rapid increase in the FC magnetic susceptibility as the temperature is decreased below ≈15 K is attributed to ordering of the Nd and Cr moments. At 300 K, the observed effective moment μ_{eff} ($\mu_{eff} = \sqrt{8\chi T}$) is 5.78 μ_B/f.u., and the paramagnetic Curie−Weiss temperature, θ (obtained from a fit of the susceptibility data between 150 and 300 K to the Curie−Weiss law), is +121 K. Leonard et al.[7] and Hartjes et al.[8] obtained similar results and assigned the low-temperature transition to an antiferromagnetic ordering of the Nd and Cr moments. Their low-temperature magnetization curves show an approach to saturation that could be interpreted as arising from antiferromagnetic exchange between the Nd and Cr sublattices (leading to ferrimagnetism), but the alternative possibility of ferromagnetic exchange could not be definitively ruled out. Neutron diffraction experiments were therefore carried out to determine the detailed magnetic structure of $NdCrSb_3$.

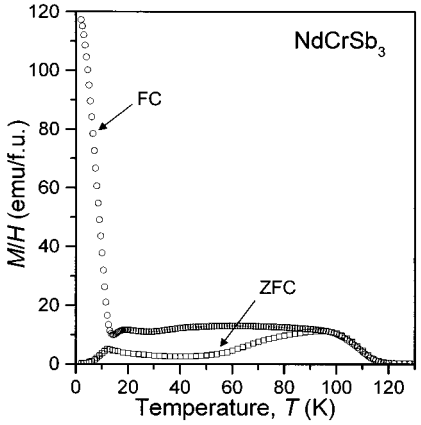

Figure 2. ZFC and FC (2 T cooling field) magnetic susceptibility (M/H) of $NdCrSb_3$ under a 100 Oe applied field.

Neutron diffraction data for $NdCrSb_3$ were collected between 4 and 130 K, encompassing both transitions observed in the magnetic susceptibility curve. Refinement details for the 4, 51, and 130 K data are collected in Table 1. The 130 K data refined well with a model based on the structure of $LaCrSb_3$.[3] The occupancy of the Cr site was found to be slightly substoichiometric,

(10) Rodriguez-Carvajal, J. *FULLPROF: A Program for Rietveld Refinement and Profile Matching Analysis*; Laboratoire Léon Brillouin (CEA-CNRS): Saclay, France, 1997.

Table 1. Profile Refinement Results for $NdCrSb_3$

temperature (K)	4			51			130		
space group	*Pbcm*			*Pbcm*			*Pbcm*		
a (Å)	12.9708(2)			12.9701(3)			12.9764(2)		
b (Å)	6.1699(1)			6.1676(1)			6.1707(1)		
c (Å)	6.0669(1)			6.0651(1)			6.0686(1)		
	x	*y*	*z*	*x*	*y*	*z*	*x*	*y*	*z*
Nd	0.3098(14)	0.0018(35)	1/4	0.3100(14)	0.0038(35)	1/4	0.3096(12)	0.0033(31)	1/4
Cr[a]	0.9077(35)	1/4	0	0.9036(37)	1/4	0	0.9059(31)	1/4	0
Sb(1)	0.0646(23)	0.1046(37)	1/4	0.0658(21)	0.1055(37)	1/4	0.0644(19)	0.1057(31)	1/4
Sb(2)	0.2209(19)	0.4931(47)	1/4	0.2209(19)	0.4960(50)	1/4	0.2204(17)	0.4984(43)	1/4
Sb(3)	0.5028(21)	1/4	0	0.5039(21)	1/4	0	0.5044(19)	1/4	0
R_{wp} (%)	6.81			6.72			5.67		
R_E (%)	3.70			3.83			3.65		
Cr moment (μ_B)	1.1			1.1(1)					
Cr moment direction	[100]			[010]					
Nd moment (μ_B)	2.6(1)								
Nd moment direction	[100]								
R_{mag} (%)	8.70			30.9					

[a] At 130 K, the Cr occupancy converged to 0.88(6). The Cr occupancy was constrained to be equal to 0.88 for the 51 and 4 K refinements.

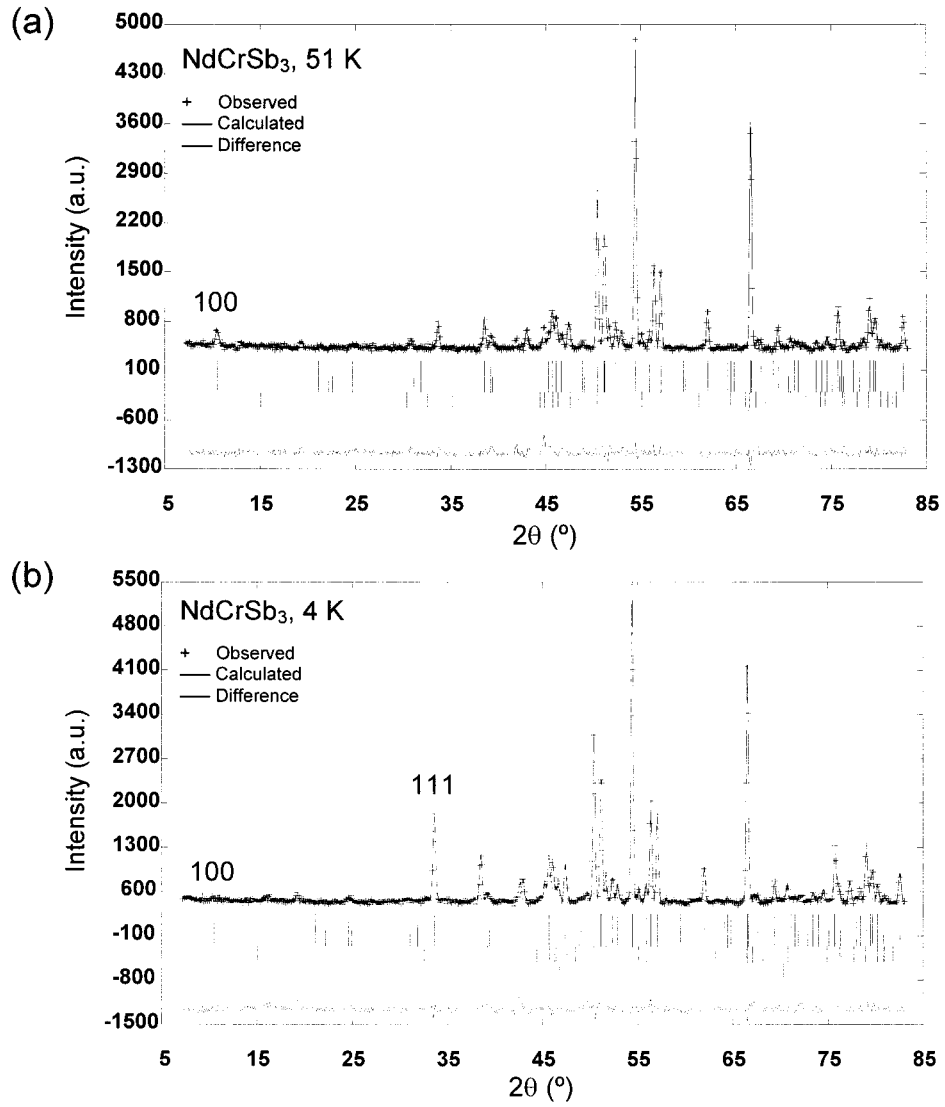

Figure 3. Rietveld refinement results for $NdCrSb_3$ at (a) 51 K and (b) 4 K. The crosses represent the observed profile, the solid line is the fitted profile, and the difference is shown at the bottom. The four sets of vertical tic marks represent the Bragg peak positions for the $NdCrSb_3$ crystal structure (top), the magnetic peak positions (second from top), and those from $NdSb_2$ (second from bottom) and CrSb (bottom) impurities.

leading to the formula $NdCr_{0.88(6)}Sb_3$. It appears that members of the $RECrSb_3$ series containing the smaller rare earths may well have a slightly lower Cr content, given that previous structure determinations have led to $LaCr_{0.95(2)}Sb_3$ and $CeCr_{0.901(9)}Sb_{2.909(4)}$.[3,4] For simplicity, however, the title compound will be referred to as $NdCrSb_3$. Rietveld refinement results at 51 and 4 K are presented in Figure 3, showing the evolution of the 100 and 111 reflections, which are the most diagnostic of the magnetic structure in this case. Figure 4 shows that

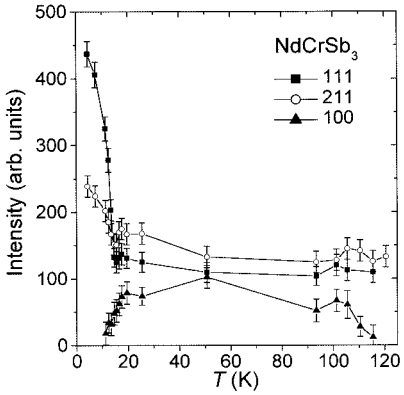

Figure 4. Temperature dependence of the 111, 211, and 100 reflections for $NdCrSb_3$. The lines are drawn only to guide the eye.

as the temperature is lowered from 130 K, the intensity of the 100 reflection increases to reach a maximum around 50 K and then decreases to zero below 15 K. The behavior between 50 and 130 K is consistent with the magnetic structure of $LaCrSb_3$ in which there is ferromagnetic ordering of the Cr moments along [010].[6] Refinement of the 51 K data showed excellent agreement with this model (Figure 3a), resulting in a Cr moment of 1.1(1) μ_B. If the Cr site is assumed to be fully occupied, the refined Cr moment is 0.9(1) μ_B, closer to that obtained for $LaCrSb_3$ (0.79(3) μ_B).[6] Even if the substoichiometry is accounted for, the value of 1.1(1) μ_B/Cr is considerably lower than what would be expected for Cr^{3+} or Cr^{4+} ions.

As the temperature is further decreased from 51 to 4 K, the disappearance of the 100 reflection and the appearance of the 111 and 211 reflections (Figures 3 and 4) indicate that the ferromagnetic model with a magnetization axis along [010] is no longer appropriate. The data at 4 K (Figure 3b) fit very well to a model in which Nd and Cr moments are ferromagnetically coupled and are oriented along a new easy magnetization axis [100]. With the Cr moment constrained to 1.1 μ_B (as obtained from the 51 K data), refinement of the 4 K data leads to a Nd moment of 2.6(1) μ_B, which is lower than that expected for Nd^{3+} ions (3.27 μ_B). The overall moment at 4 K is then 3.7(1) μ_B. The 4 K data also display a reflection near 42.5° that is significantly broader than the other reflections, which leads to a peak in the difference plot (Figure 3). This reflection has a very different temperature dependence than the magnetic ones; the intensity is essentially temperature independent from 4.3 to 25.3 K and reaches zero by 51 K. There is no magnetic anomaly in this temperature range in either the dc or ac susceptibility, so it can be concluded that this peak is not related to changes in the magnetic structure of $NdCrSb_3$. Attempts were made to index the 42.5° reflection on several possible impurity phases, such as $NdSb_2$, Nd_2Sb, and Nd_5Sb_3, but the results were ambiguous at best. This reflection also indexes approximately as 1 1 $^3/_2$ on the $NdCrSb_3$ cell, which suggests the possibility of a low-temperature structural phase transition in this material. There are no X-ray data available in this temperature range. At present, no definitive conclusion can be made regarding the origin of this peak in the neutron data.

To reiterate, the neutron diffraction studies support a magnetic structure in which, as the temperature is

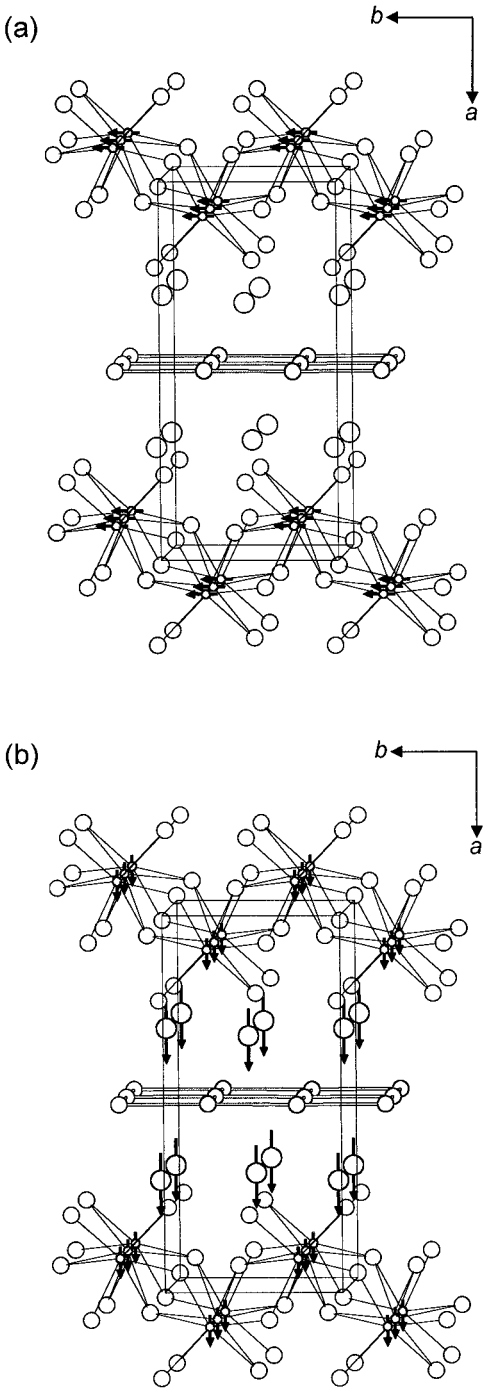

Figure 5. Representation of the magnetic unit cell of $NdCrSb_3$ (a) at 51 K with ferromagnetically ordered Cr moments along [010] and (b) at 4 K with ferromagnetically ordered Nd and Cr moments along [100].

decreased, the Cr moments first undergo ferromagnetic ordering along [010] and then flip to a new direction [100] upon ferromagnetic coupling with the Nd moments. This is illustrated in Figure 5. The ordering temperatures T_C were determined here by ac magnetic susceptibility measurements. The maxima in the χ'_{ac} (in-phase) magnetic susceptibility (Figure 6) pinpoint the long-range ordering temperature for the Cr moments at $T_C(Cr) = 107.8$ K and for the Nd and Cr moments together at $T_C(NdCr) = 12.7$ K. The χ''_{ac} (out-of-phase) magnetic susceptibility (inset of Figure 6) also displays corresponding maxima at 105.5 and 10.7 K, consistent with the generation of a spontaneous moment upon

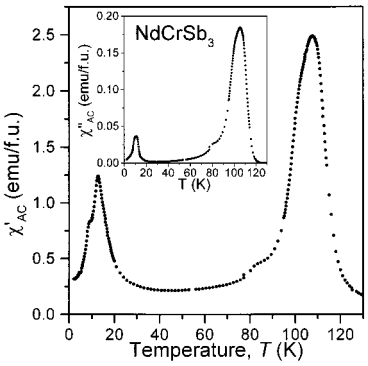

Figure 6. χ'_{ac} and (inset) χ''_{ac} magnetic susceptibility of $NdCrSb_3$ between 2 and 130 K ($H_{dc} = 0$).

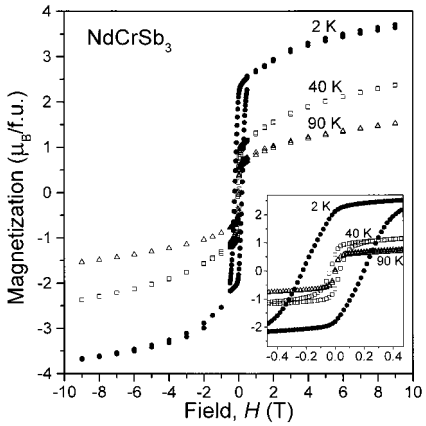

Figure 7. Isothermal hysteresis loops for $NdCrSb_3$ at 2, 40, and 90 K.

long-range ferromagnetic ordering. The ordering temperatures obtained here are similar to those previously reported (T_C(Cr) = 141 K or 122(4) K; T_C(NdCr) = 18 K or 11(3) K),[7,8] with T_C(Cr) being somewhat lower than the literature values. These discrepancies probably arise from differences in Cr stoichiometry or from the method of determining T_C, which were found here in the absence of an applied dc field. $NdCrSb_3$ also has a lower T_C(Cr) than $LaCrSb_3$ (125 K);[6] the substoichiometry of Cr in $NdCrSb_3$ likely plays an important role in the decrease of the long-range ordering temperature of the Cr sublattice. Neither of the ac susceptibility maxima showed a dependence on the frequency in the range 10−1000 Hz. The small shoulder in the χ'_{ac} plot at ≈9 K (Figure 6) does not have an associated χ''_{ac} component (inset of Figure 6) and is possibly due to the presence of $NdSb_2$, which undergoes antiferromagnetic ordering at low temperatures.

Figure 7 shows the field dependence of the magnetization up to 9 T at 2, 40, and 90 K. At 2 K, the magnetization approaches saturation with $M_{9T} = 3.70$ μ_B/f.u., in excellent agreement with the overall moment (3.7(1) μ_B) determined from the neutron diffraction data at 4 K. At the higher temperatures (where T_C(NdCr) < $T < T_C$(Cr)), the saturation magnetizations are 2.37 and 1.55 μ_B/f.u. at 40 and 90 K, respectively. Coercive fields of 2100 and 400 Oe and remanent magnetizations of 2.2 and 0.8 μ_B/f.u. are observed for the hysteresis loops at 2 and 40 K, respectively, while the magnetization at 90 K is anhysteretic. The coercive field at 40 K is very close to that for $LaCrSb_3$ ($H_C = 450$ Oe),[8] which is due solely to ordered Cr moments. The significant increase in the

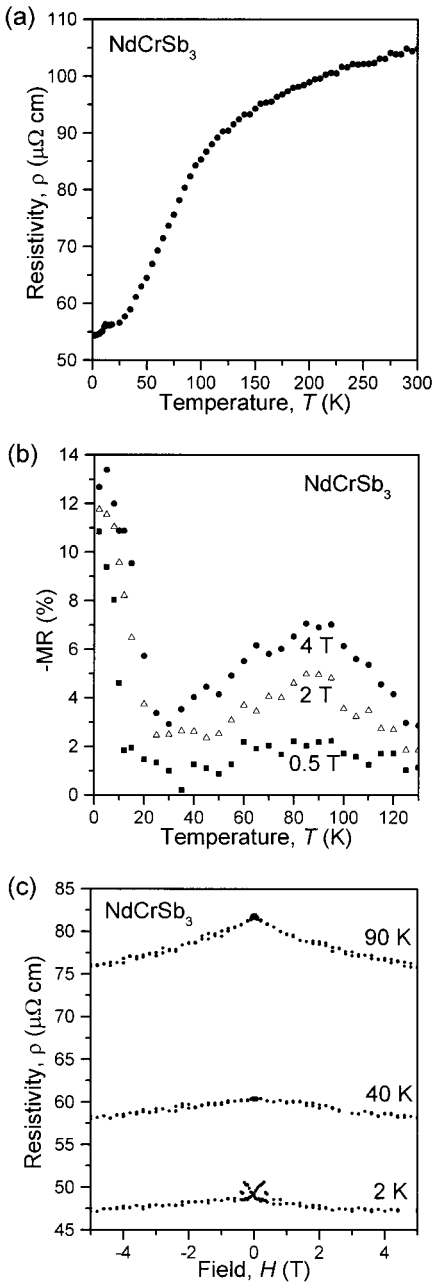

Figure 8. (a) Temperature dependence of the electrical resistivity under a zero applied field. (b) Magnetoresistance between 2 and 130 K at fields of $H = 0.5$, 2, and 4 T. (c) Field dependence of magnetoresistance at 2, 40, and 90 K. The resistivities were measured on a single crystal of $NdCrSb_3$ parallel to the *c* axis and the fields were applied perpendicular to this axis.

coercive field at 2 K for the ordered ferromagnetic Nd/Cr lattice originates from the magnetocrystalline anisotropy of Nd arising from important spin−orbit coupling in rare-earth elements.

The Cr moment of 1.1 μ_B (at 51 K) determined from neutron diffraction data is considerably lower than expected for any reasonable formal Cr oxidation states, such as Cr^{3+} ($3d^3$, ≈3.0 μ_B) or Cr^{4+} ($3d^2$, ≈2.0 μ_B). Like $LaCrSb_3$, where a low saturation magnetization was also observed ($M_{5T} = 0.8$ or 1.0 μ_B/f.u.)[6,8] and where the Fermi level crosses nearly filled, narrow Cr-based bands in the density of states,[6] $NdCrSb_3$ is interpreted as being a band ferromagnet, with the deviation from the free-ion values occurring because of the nonlocalized nature

of the Cr moments. Taking into account a Cr moment of 1.1 μ_B, the Nd moment is found to be 2.6 μ_B, not as high as expected for Nd^{3+} ions (3.27 μ_B/Nd^{3+}; $g_J = 8/11$, $J = 9/2$). This cannot be accounted for by antiferromagnetic ordering between Cr and Nd moments, producing a ferrimagnet, as this was not observed by neutron diffraction. Such a reduction in Nd moment, however, is frequently observed in rare-earth intermetallic compounds at low temperatures and is attributed to the crystalline electric field resolving the ground multiplet $^4I_{9/2}$.[11]

Resistivity and Magnetoresistance. $NdCrSb_3$ exhibits metallic behavior, as shown in the resistivity curve (Figure 8a), which resembles a previous zero-field measurement.[7] In the presence of various applied fields, $NdCrSb_3$ exhibits negative magnetoresistance (MR(%) $= [(\rho(H) - \rho(0))/\rho(0)] \times 100$), reaching maximum values just below the two ordering transitions (Figure 8b). When the applied field is 4 T, the magnetoresistance MR is −7% at 95 K (below T_C(Cr)) and reaches its extremum of −13% at 5 K (below T_C(NdCr)). Studies on $LaCrSb_3$ in which only the ordering of the Cr moments can affect the sample resistivity led to a MR of ca. −6% at 150 K and 5 T.[9] Isothermal magnetoresistance data at 2, 40, and 90 K (Figure 8c) disclose the field dependence of the resistivity upon ordering of the Cr and Nd/Cr lattices. The negative MR observed in all cases is consistent with both ordering transitions being ferromagnetic. Only the 2 K plot displays hysteresis upon cycling the field to 5 T; the coercive field of ≈0.3 T is similar to that observed in the magnetization experiment.

(11) Szytuła, A., Leciejewicz, J., Eds. *Handbook of Crystal Structures and Magnetic Properties of Rare Earth Intermetallics*; CRC Press: Boca Raton, FL, 1994.

Acknowledgment. Financial support from the Natural Sciences and Engineering Research Council of Canada is gratefully acknowledged. We thank Christina Barker for assistance with the EDX analyses. We thank Dr. I. Swainson and Mr. R. Donaberger of the Neutron Program for Materials Research of the National Research Council of Canada for assistance with the neutron diffraction experiments.

CM001405L